iScience

CellPress
OPEN ACCESS

Article

Electrically synchronizing and modulating the dynamics of ERK activation to regulate cell fate

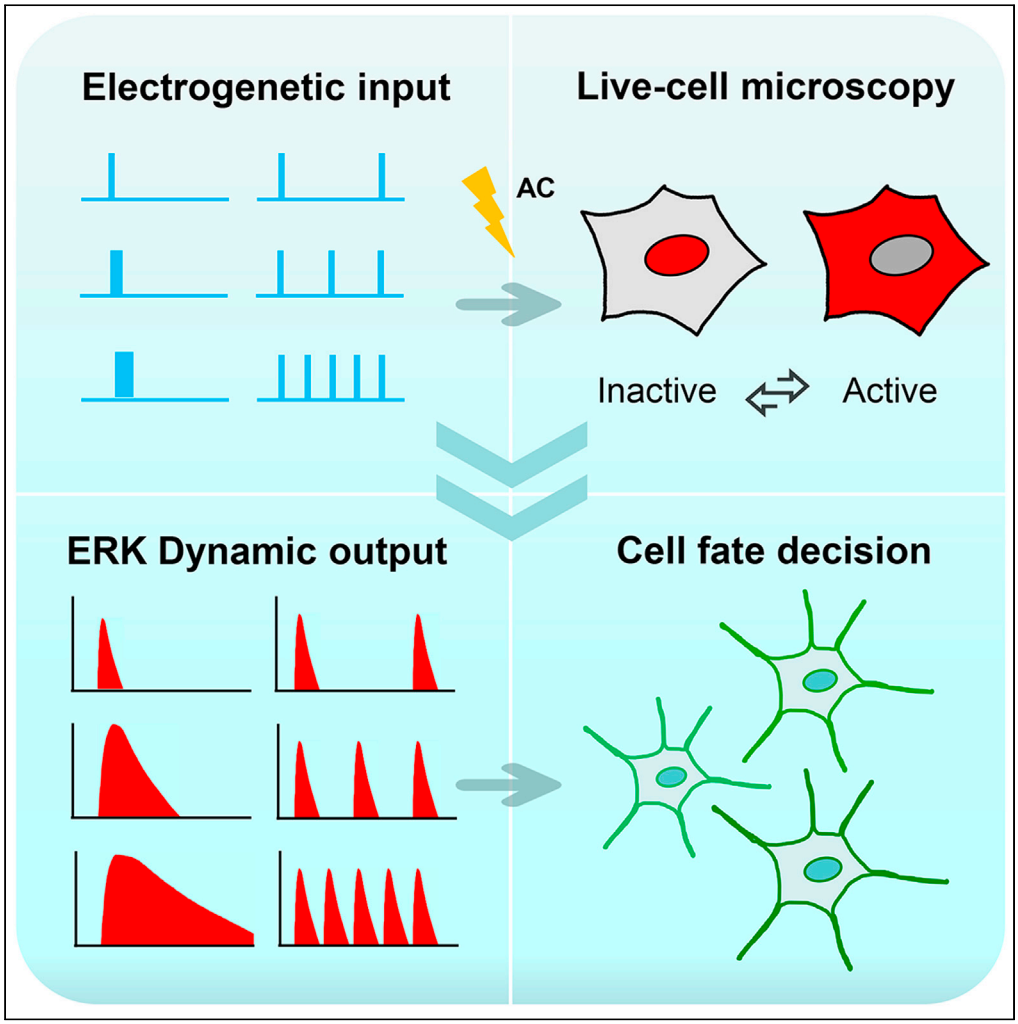

Liang Guo, Kan Zhu, Michael Pargett, ..., Wolfgang Losert, John Albeck, Min Zhao

minzhao@ucdavis.edu

Highlights

Alternating-current (AC) electric field activates ERK independently of growth factors

AC stimulation length modulates the amplitude and duration of ERK activation

On-off time interval of AC modulates the frequency of ERK activation peaks

Electrical modulation of ERK dynamics promotes neuronal differentiation of PC12 cells

Guo et al., iScience *24*, 103240
November 19, 2021
https://doi.org/10.1016/j.isci.2021.103240

iScience

CellPress
OPEN ACCESS

Article

Electrically synchronizing and modulating the dynamics of ERK activation to regulate cell fate

Liang Guo,[1,2,6] Kan Zhu,[1,6] Michael Pargett,[3] Adam Contreras,[1] Patrick Tsai,[1] Quan Qing,[4] Wolfgang Losert,[5] John Albeck,[3] and Min Zhao[1,7,*]

SUMMARY

Intracellular signaling dynamics play fundamental roles in cell biology. Precise modulation of the amplitude, duration, and frequency of signaling activation will be a powerful approach to investigate molecular mechanisms as well as to engineer signaling to control cell behaviors. Here, we showed a practical approach to achieve precise amplitude modulation (AM), frequency modulation (FM), and duration modulation (DM) of MAP kinase activation. Alternating current (AC) electrical stimulation induced synchronized ERK activation. Amplitude and duration of ERK activation were controlled by varying stimulation strength and duration. ERK activation frequencies were arbitrarily modulated with trains of short AC applications with accurately defined intervals. Significantly, ERK dynamics coded by well-designed AC can rewire PC12 cell fate independent of growth factors. This technique can be used to synchronize and modulate ERK activation dynamics, thus would offer a practical way to control cell behaviors *in vivo* without the use of biochemical agents or genetic manipulation.

INTRODUCTION

Intracellular signaling is a highly dynamic process. Importantly, the dynamics encode distinct information for transcription of specific genes and for the induction of critical cellular responses. Like information encoded by radio signals, frequency modulation (FM) and amplitude modulation (AM) of a signaling pathway instruct cells to carry out distinct and specific tasks (Deneke and Di Talia, 2018; Micali et al., 2015). AM, FM, and duration modulation (DM) of activation of the same signaling pathways and transcription factors have been demonstrated to code specific and different information for cells both *in vitro* and in *vivo* (Albeck et al., 2013; Hansen and O'Shea, 2013, 2016; Hao and O'Shea, 2011; Ryu et al., 2015; Toettcher et al., 2013; Wilson et al., 2017).

The dynamics of intracellular signaling determine the decision to progress through the cell cycle. When a population of cells is exposed to extracellular stimulation, such as increases of growth factors, Extracellular-signal Regulated Kinase (ERK) is activated in most cells. Then individual cells start to show discrete, asynchronous oscillations of ERK activation with highly heterogeneous frequency, amplitude, and duration, even in the same and well-controlled extracellular concentrations of growth factors (Albeck et al., 2013; Ryu et al., 2015; Sparta et al., 2015; Toettcher et al., 2013; Wilson et al., 2017). Eventually, even in genetically identical sister cells subjected to the same concentration of growth factor stimulation, cell-to-cell variability in ERK signaling dynamics influences the decision to enter the S phase in that same environment (Albeck et al., 2013).

Signaling dynamics affect cell fate determination. Different activation dynamics of the same signaling pathway, such as ERK, result in very different cell responses (Albeck et al., 2013; Allan et al., 2003; Klemke et al., 1997; Lai et al., 2001; Luciano et al., 2003; Roux and Blenis, 2004; Ryu et al., 2015; Wortzel and Seger, 2011). Both neural growth factor (NGF) and epidermal growth factor (EGF) activate ERK in PC12 cells (a cell line derived from rat pheochromocytoma). NGF induces prolonged ERK activation and eventually induces differentiation of the cells with neurite-like process growth. In contrast, EGF induces transient ERK activation, and eventually increases cell proliferation (Murphy et al., 2002).

[1]Department of Ophthalmology & Vision Science, Department of Dermatology, Institute for Regenerative Cures, University of California, Davis, Sacramento, CA 95817, USA

[2]College of Intelligent Systems Science and Engineering, Harbin Engineering University, Harbin, Heilongjiang 150001, China

[3]Department of Molecular and Cellular Biology, University of California Davis, Davis, CA 95616, USA

[4]Department of Physics, Biodesign Institute, Arizona State University, Tempe, AZ 85287, USA

[5]Department of Physics, Institute for Physical Science and Technology, University of Maryland, College Park, MD 20742, USA

[6]These authors contributed equally

[7]Lead contact

*Correspondence: minzhao@ucdavis.edu

https://doi.org/10.1016/j.isci.2021.103240

Significantly, a growing body of literature supports the relevance of temporal coding in transcriptional regulation, where information from various environmental signals is encoded in the temporal dynamics of the shared transcription factor, intracellular signaling in development, wound healing, and cancer (Behar and Hoffmann, 2010; Bugaj et al., 2018; Hansen and O'Shea, 2016; Purvis and Lahav, 2013; Ravindran and Wilson, 2018).

Therefore, the ability to induce - synchronized across cell groups - activation of signaling pathways with controlled frequency, amplitude, and duration will provide a powerful research tool to elucidate temporal encoding mechanisms. Ryu et al. developed an elegant microfluidics device, which showed remarkable control of cell fate by periodical addition and wash-out of growth factors in a cell culture chamber (Ryu et al., 2015). Toettcher et al. took advantage of optogenetics and interrogated the dynamic control of signal transmission by the Ras/Erk module (Toettcher et al., 2013). Optogenetic control of ERK activation dynamics is also used successfully to control cell migration (Aoki et al., 2017).

Here, we present a very practical approach to induce precisely synchronized frequency, amplitude, and duration of ERK activation. By modulating these signaling dynamics, we are able to control cell fate. Importantly, we believe that our technique has several advantages over optogenetic and microfluidic methods to achieve synchronized FM, AM, and DM, and combinations of those dynamic parameters for translatable *in vivo* and eventually clinical applications, because electrical stimulation is much easier to apply *in vivo* and in clinical situations.

To establish a complete set of AC stimulation schemes to control intracellular signaling dynamics, we subjected an MCF10A cell line that has a stable expression of an ERK reporter to different voltages, AC frequencies, AC waveforms, stimulation durations, and stimulation on/off patterns (Figure 1A). We selected ERK reporter ERKTR because of its dynamic's fidelity in reflecting activation and deactivation (Albeck et al., 2013; Hansen and O'Shea, 2013, 2016; Hao and O'Shea, 2011; Ryu et al., 2015; Toettcher et al., 2013; Wilson et al., 2017) (Figure 1B), which allows quantitative interrogation of the dynamics of ERK activation (Figure 1C). Upon achievement of precise synchronization modulation of frequency, amplitude, duration, and their combinations for ERK activation, we set to test the effects of controlled ERK activation dynamics on cell fate determination, i.e., differentiation in PC12 cells with designed electrical stimulation schemes and FM and AM of ERK activation (Figure 1D).

RESULTS AND DISCUSSION

Continuous electrical stimulation induced ERK activation

To activate ERK signaling, we first subjected MCF10A cells that express ERKTR, an ERK translocation reporter, to continuous AC electrical stimulation in a custom-made stimulation device (Figures 2A and 2B). ERKTR contains tandem nuclear import and export sequences juxtaposed with an ERK phosphorylation motif, enabling it to report ERK activity as the ratio of cytosolic fluorescence (Fc) to nuclear fluorescence (Fn) (Pargett et al., 2017; Regot et al., 2014).

Upon AC stimulation, ERKTR translocated from the nucleus to the cytosol, indicating an increase in ERK activity (Figure 2C; Video S1) (Pargett et al., 2017). ERK activation of each cell can be quantified along time (Figures 2C and 2D), with activation peaks automatically identified by our software (Figure 2F). ERK activation in individual cells, and the population average, peaked at about 15 min following AC stimulation (Figures 2D–2G). Cells subjected to continuous AC stimulation of 1 h showed a gradual decrease of ERK activation (Video S1; Figures 2D–2G).

We then used EGF to verify the activation of ERK. Addition of EGF induced ERKTR translocation from the nucleus to the cytosol. Gefitinib (an EGFR inhibitor) abolished the effect of EGF (Figure S1). Quantification of EGF-induced ERK activation in individual cells and in a population of cells confirmed the suitability of electric stimulation for ERK activation dynamics interrogation (Figures S1B–S1E). ERK activation induced by EGF was consistent with that reported before (Albeck et al., 2013). EF-induced ERK activation is further analyzed using k-means clustering with squared Euclidean distance. Three clusters of representative temporal activation patterns were found, which is very similar to that induced by EGF stimulation (Ryu et al., 2015) (Figure S2). Despite different pre-stimulation ERK activation levels (Figures S2A–S2E), upon field-onset, all three clusters showed simultaneous and similar time-to-peak, peak amplitude, peak-to-peak amplitude, and convergence to the same activation level after 30 min (Figure S2). AC stimulation thus

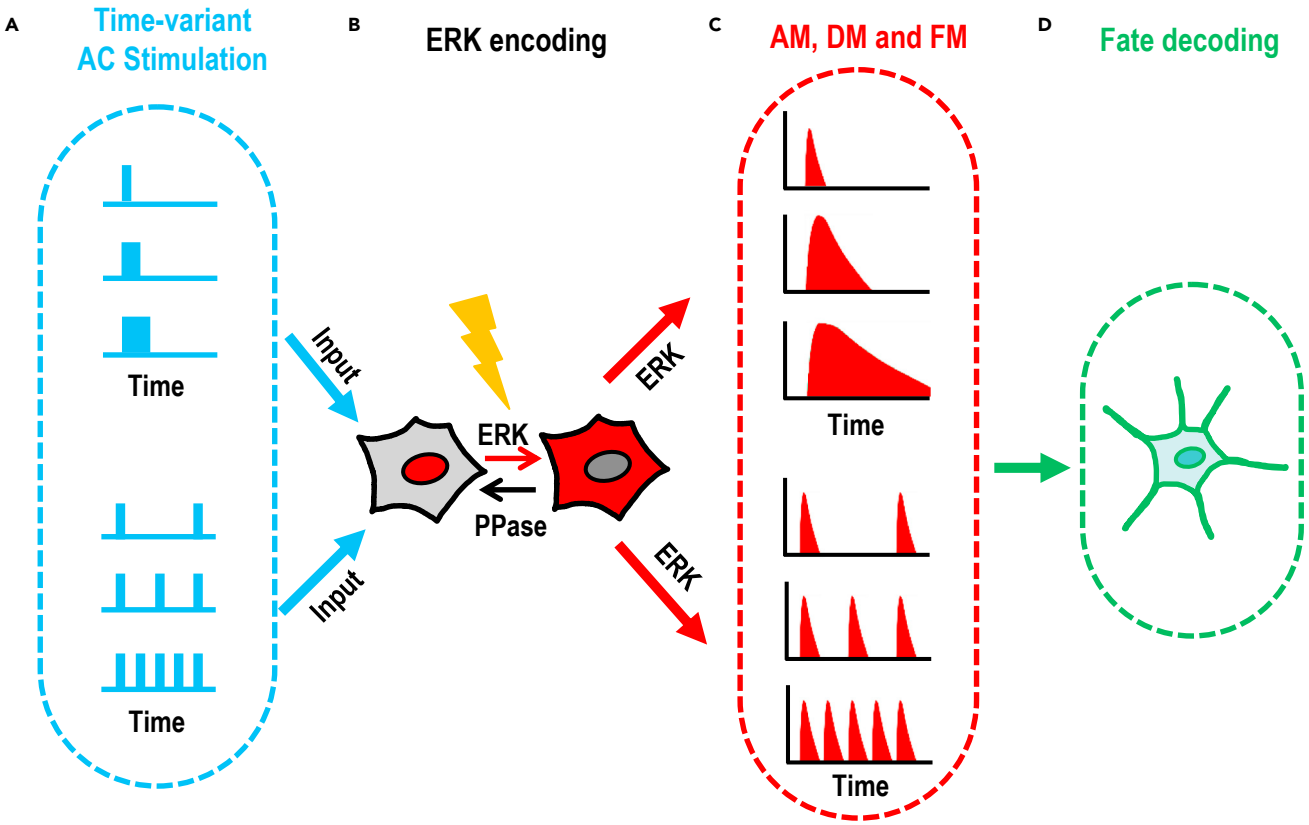

Figure 1. Schematic diagram shows experimental design to test the hypothesis that electrical stimulation induces precision amplitude modulation (AM), duration modulation (DM), and frequency modulation (FM) of ERK activation, which in turn may regulate cell behaviors

(A) Time-variant AC Stimulation.

(B) ERK translocation reporter dynamically reports ERK activation.

(C) The voltage, duration, and repetition of AC stimulations induce amplitude modulation (AM), duration modulation (DM), and frequency modulation (FM) of ERK activation.

(D) Signaling encoded in AM, DM, and FM of ERK dynamics rewires cell fate.

synchronized these three clusters of cells in the activation dynamics. Therefore, ERK activation induced by EF and EGF, including the dynamics of Fc/Fn ratio are comparable to each other (Figure 2 and Video S1, compared to Figure S1 and Video S2).

Short-term AC modulated amplitude and duration of ERK activation

We next changed stimulation duration (i.e., on-time) to achieve more precise control of ERK activation peak, overall amplitude, and duration (Figures 3 and S3, and Video S3). AC stimulation of 28 V/cm, 500Hz for 1 min (1′) did not induce noticeable ERK activation (Figure 3A). 2 min (2′) AC stimulation (28V/cm, 500Hz) elicited a robust ERK activation response peaking around 13 min following the onset of stimulation. The ERKTR ratio (Fc/Fn) quickly returned to the pre-stimulation level at about 15′–20′ (Figure 3B). Stimulation for 3′ induced a stronger and longer lasting ERK activation peak then gradually returned to the basal level around 90 min after stimulation (Figure 3C). Stimulation for 5′ induced a sustained ERK activation, lasting over 90 min with a slight decline in the overall ERK activation level. The ERK activation peak appeared at the same time and with the same peak value as the following 3′ stimulation (Figure 3D). AC stimulation of 3′ and 5′ evoked similar mean ERK activation amplitudes, whereas 2′ AC stimulation induced lower mean amplitudes. 2′, 3′, and 5′ induced short, medium, and long duration of ERK activation, respectively (Figure 3E). The ERK activation peak occurred about 2 min earlier in short AC stimulation pulses when compared to that in continuous AC of the same voltage (Figure 3B). To further confirm electric stimulation induced ERK activation, we tested a different reporter system, FRET-based reporters, EKAR3. ERKTR and cytosolic EKAR3 were co-expressed in MCF10A cells (Figure S5). Both reporters responded

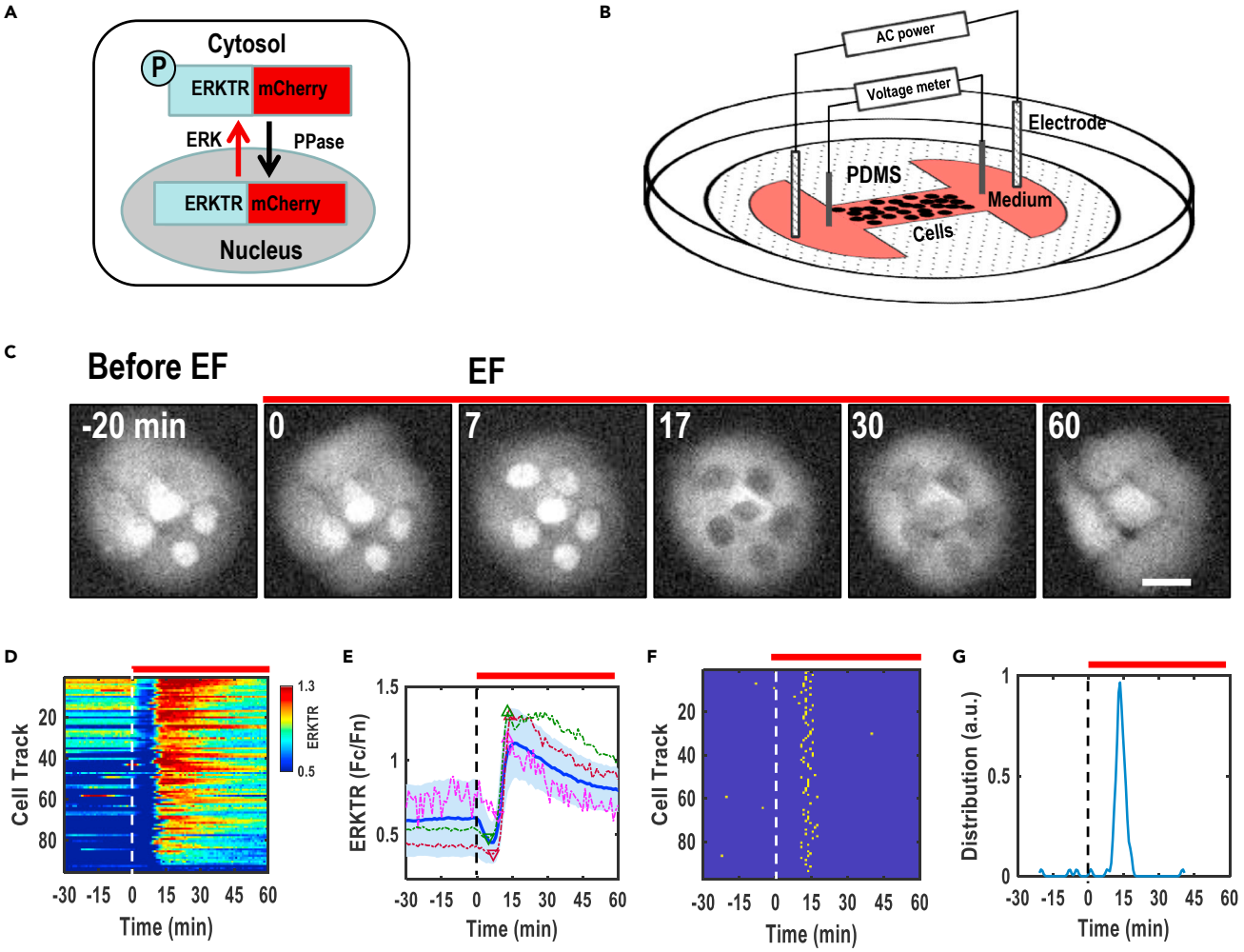

Figure 2. AC electrical stimulation induced robust ERK activation

(A) Schematic of ERK translocation reporter (ERKTR-mCherry) that shuttles between the cytosol and nucleus upon activation and inactivation of ERK, respectively.

(B) Schematic of the AC stimulation device. Global AC EFs were applied to cells in the chamber through Ag/AgCl electrodes.

(C) Representative time-lapse fluorescence images of MCF10A cells expressing ERKTR. Cells were starved in serum-free imaging medium, and then exposed to AC stimulation continuously as indicated. ERKTR is translocated from the nucleus to the cytosol, reporting the activation of ERK.

(D) Composite heatmap of the time courses of ERK activities as quantified by Fc/Fn. Each horizontal line represents the ERK activity time course of one single cell (n = 97 cells). The vertical dotted line indicates the application of AC (t = 0).

(E) Population responses of ERK activity. Thick blue line indicates the mean ERKTR ratio from a population of 97 cells with a light blue shade showing the standard deviation range (SD). Three randomly selected single cell-ERK trajectories are also shown (dotted lines), triangles/inverted triangles indicate the peaks/valleys of ERK traces which are identified with an algorithm that compares data traces rise/fall beyond the threshold.

(F) Peak map showing ERK activation peaks identified automatically from the ERK traces of d. Each row represents one cell. Each yellow dot indicates one identified ERK peak.

(G) The peak points from f. were collected to quantify peak distribution. Note: horizontal red bars indicate the duration of AC stimulation. EF = 28V/cm (RMS), 500Hz, bipolar square wave. Scale bars, 20 μm.

to AC-stimulation. EKAR3 typically peaked at 10-15 min and then declined in 30 min, while ERKTR peaked at 15 min and maintained a plateau for over 1 h. It's worth noting that a slight but noticeable decrease in Fc/Fn occurred soon after the AC stimulation application before the robust ERK activation (Figures 2E and 3B–3D). Moreover, AC stimulation induced two or more ERK peaks in some of the cells (Figure S4).

To determine the effects of different voltages, frequencies, duty cycles, and waveforms on AC induced ERK activation, we varied those parameters and evaluated the ERK activation dynamics on MCF10A cells. Cells were stimulated for 3 min, and representative results are presented here, including different voltages

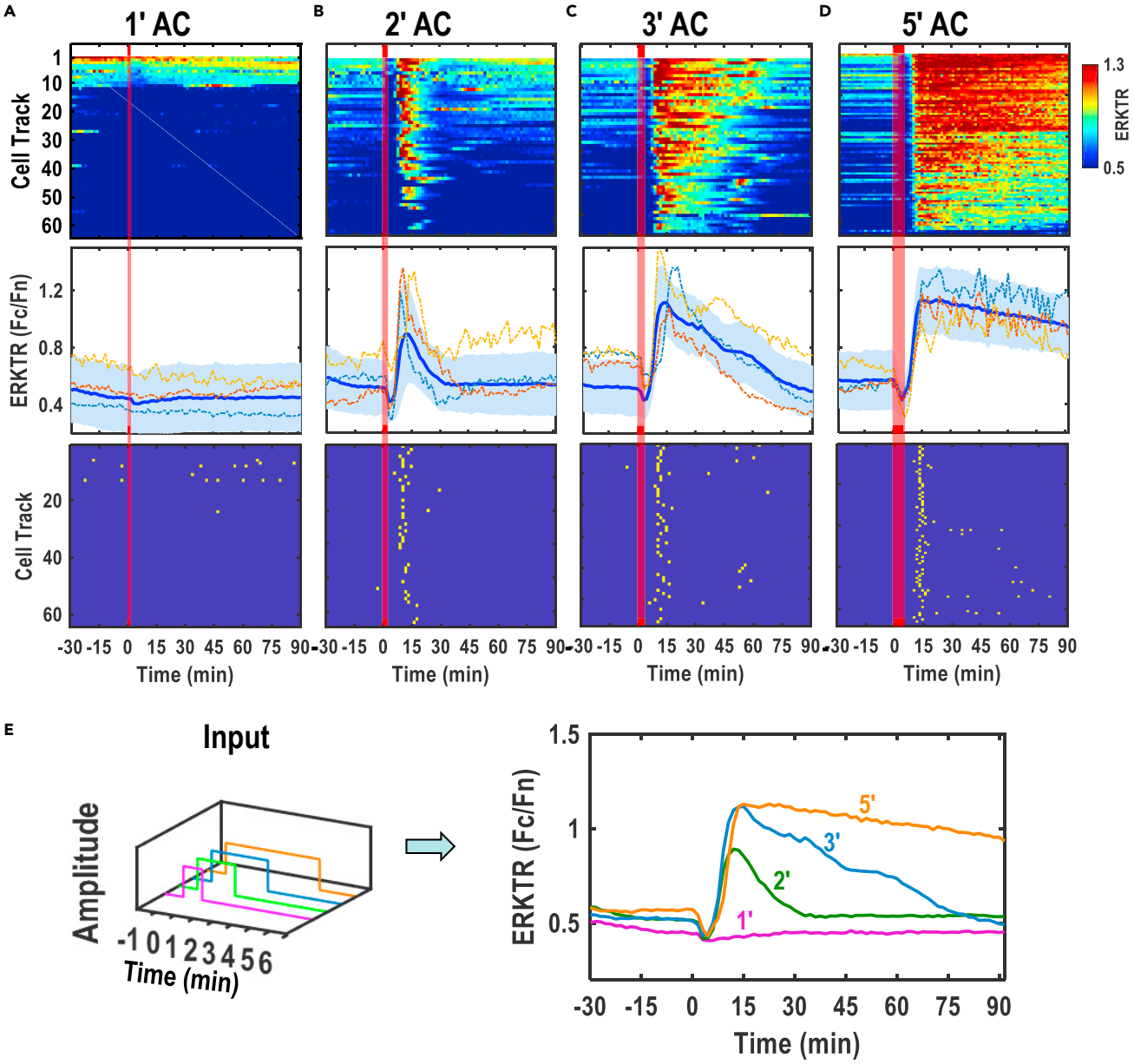

Figure 3. Short AC stimulation modulated the amplitude and duration of ERK activation

Representative ERK dynamics with different AC stimulation duration are displayed in 3 ways: Heatmaps which shows individual ERK activation traces by each row, average ERK activation in blue lines with standard deviation in the shade (n > 100), and peak maps in which the peaks identified from the ERK traces.

(A) 1′ AC stimulation did not trigger ERK activation or the peaks of ERK activation.

(B) 2′ AC stimulation gave rise to adaptive responses of ERK activation, and several peaks were generated shortly after AC stimulation.

(C) 3′ AC stimulation induced stronger responses of ERK activation, and most of the peaks were generated shortly after AC stimulation and lasted longer.

(D) 5′ AC stimulation elicited sustained responses of ERK activation, and more peaks were generated after AC stimulation with synchronous activations.

(E) Overlaid average ERK activation dynamics demonstrate that the length of AC stimulation modulates both amplitude and duration of ERK activation.

Note: Red bars indicate the duration of AC stimulation. 28V/cm, 500Hz and bipolar square wave.

(20 V/cm, 24 V/cm, and 28 V/cm), frequencies (50 Hz and 500 Hz), duty cycles (100% and 50%) and waveforms (square/triangular). At the same root mean square (RMS) voltage, magnitudes of duty cycle, and waveforms were varied (Figures S6A, S6E, S6I, S6L, S6O, and S6Q). Stimulation of RMS voltage at 28 V/cm of all waveforms and duty cycles induced robust ERK activation (Figures S6F, S6G, S6H, S6M, S6N, and S6Q). Stimulation at 20 or 24 V/cm of RMS voltage did not trigger ERK activation (Figures S6B, S6C, S6D, S6J, S6K, and

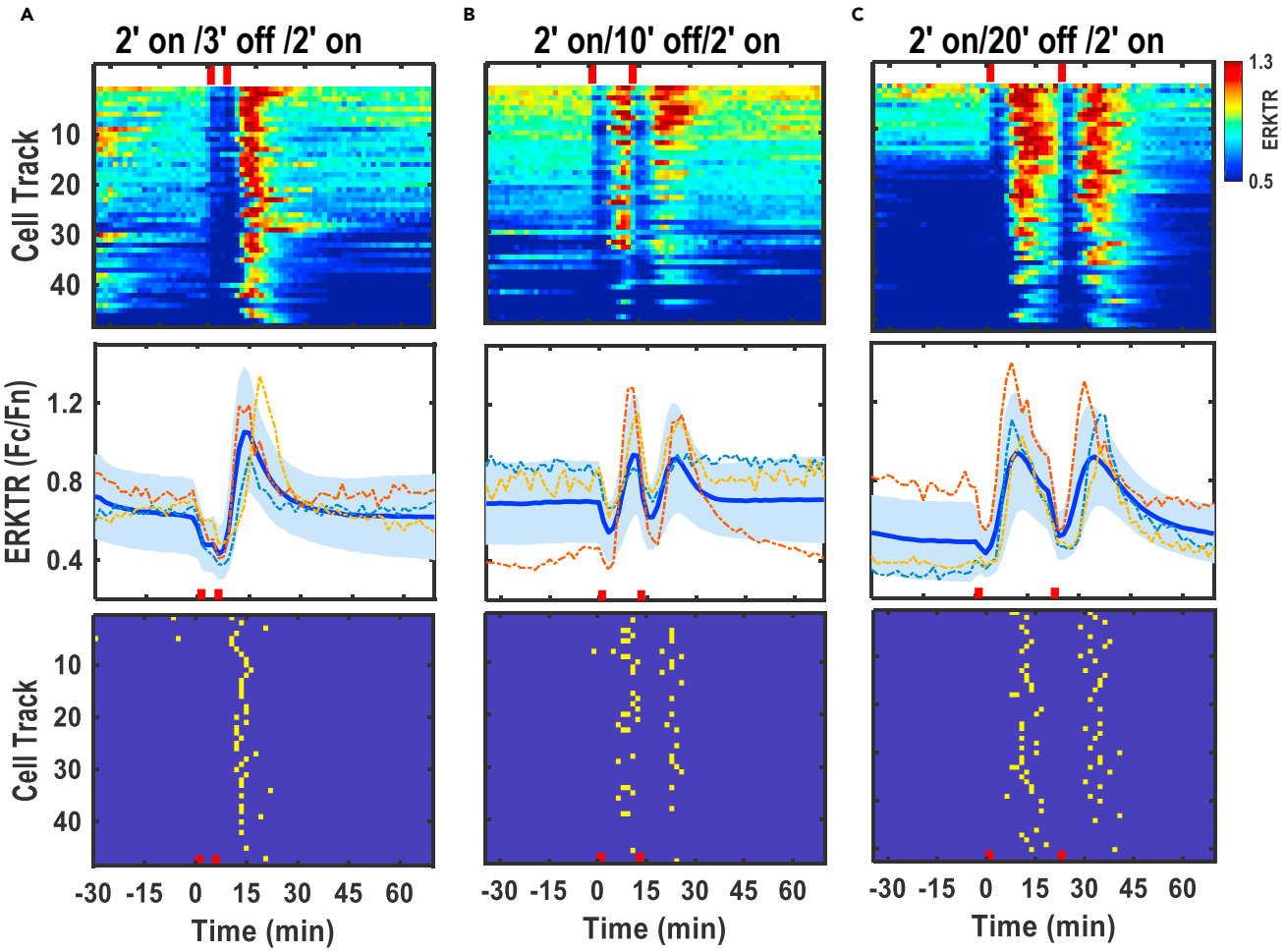

Figure 4. Optimization of AC stimulation interval to induced consecutive ERK activation wave

(A) Two Consecutive 2′ AC stimulation with a 3′ interval (2′ on/3′ off/2′ on) induced synchronous ERK activation (top panel). Only one ERK activation peak can be identified based on the population average curve (middle panel, thick blue line) with standard deviation in light blue shade and peak map (lower panel) of ERK activation.

(B) AC stimulation with 2′ on/10′ off/2′ on induced two well separated ERK activation waves (middle panel) with distinct activation peaks (lower panel).

(C) 2′ on/20′ off/2′ on AC stimulation induced two parallel ERK activation waves with similar peak values, duration and ascending and descending time courses (middle panel) and comparable peak distribution (lower panel). Note: red bar indicates the delivery of AC stimulation.

S6P). The voltage, therefore, appears to be the primary factor to induce ERK activation. All stimulations of 3′ showed very similar peak distributions (Figures S7 and S4). ERK activation lasted for varied periods depending on input voltage and duration of stimulation.

Consecutive twice delivery of AC stimulation on ERK activation

To determine the ERK response to a second AC stimulation, we chose the 2′ stimulation pattern because the ERKTR ratio will return to the basal level quickly after the 1st activation peak, which allows for easy identification of a second peak following a second stimulation (Figure 3B). We thus delivered the 2nd AC stimulation of 2′ duration (500Hz, 28V/cm) at various intervals following the 1st delivery (Video S4). When 2 short AC stimulations were delivered with an interval of 3 min or less, only one single ERK activation peak could be detected (Figures 4A, S8A, and S9A). The peak of ERK activation occurred soon after 2nd stimulation was delivered.

When the 2nd stimulation was delivered 10 min after the 1st stimulation, a comparable 2nd ERK activation peak was induced (Figures 4B, S8B, and S9B, and Video S4). When the 2nd stimulation was delivered 20′

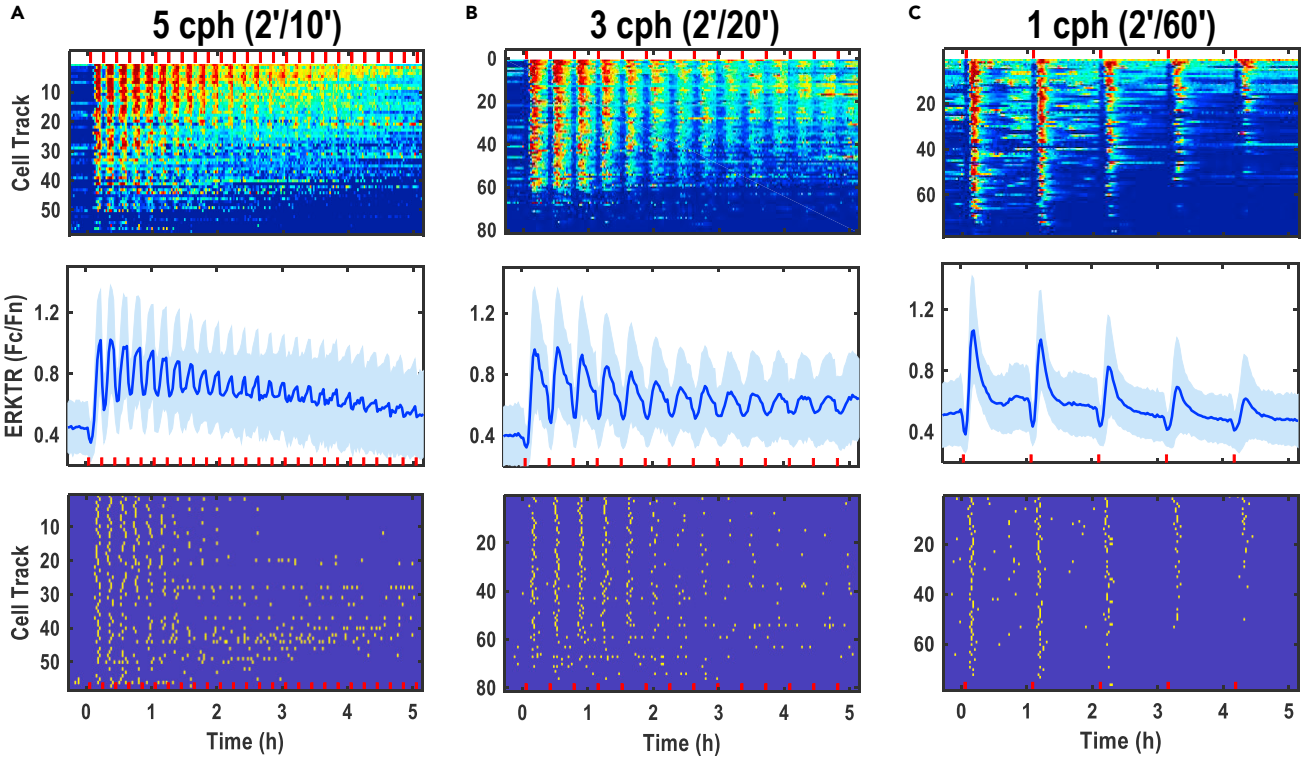

Figure 5. Trains of AC stimulation induced robust ERK activation and precisely synchronized frequency

AC stimulation of 2′ duration with a wide range of intervals from 10′ and longer induced synchronized frequency modulation (FM) of ERK activation. Synchronized oscillations of ERK activation at frequencies are shown with 5, 3, and 1 cycle(s) per hour (cph). ERK activation data are displayed in three ways: heatmaps show individual ERK activation trajectories (upper panels), average ERK activation with standard deviation in the shade (n > 50) (middle panels), and peak maps in which the peaks are identified from the same ERK traces of heatmaps (lower panels).

(A) Train stimulation of 2′ on/10′ off induced robust and synchronized ERK activation oscillation of 5 cph. The synchronized ERK activation oscillation appeared to persist up to 4-5 h

(B) Train stimulation of 2′ on/20′ off elicited a synchronized ERK activation oscillation of 3cph remained evident up to 5 h

(C) Train stimulation of 2′ on/60′ off elicited a synchronized ERK activation oscillation of 1cph with distinct ERK peaks over 4 h or longer. Note: 28V/cm, 500Hz, and bipolar square waves are indicated by red bars at the bottom of each panel.

after the 1st stimulation, the two ERK activation peaks were well separated (Figures 4C, S8C, and S9C, and Video S4). Those experiments thus suggested that optimal electrical stimulation schemes are important for the precise modulation of the frequency of ERK activation waves.

Elegant experiments using EGF and NGF pulse stimulation demonstrated that due to a refractory period for ERK activation in the MAP kinase network structure, ERK re-activation requires a period of time to recover after the first activation (Ryu et al., 2015). Our results indicated that AC stimulation, different from growth factor stimulation, may induce 2nd ERK activation peak even when ERK activation was still occurring in or shortly after the peak (Figures 4B and 4C).

Modulation and synchronization of ERK activation by trains of short AC stimulation

To modulate the frequency of ERK activation for an extended period of time, we designed and used trains of AC stimulation from selected parameters. Indeed, a train of 2′ on-10′ off induced oscillations of ERK activation at a high amplitude in a highly synchronized manner (Figures 5A and S10A, and Video S5). The frequency of ERK activation was modulated at 5 cycles per hour (cph), and the synchronized ERK activation oscillations lasted for 4-5 h. While the amplitude of individual ERK activation peaks was getting smaller, the number of identified peaks became fewer.

Trains of 2′ on-20′ off and 2′ on-60′ off, triggered very distinct ERK activation peaks, with robustly defined oscillation frequencies of 3 cph and 1 cph (Figures 5B, 5C, S10B, and S10C, and Videos S6 and S7). Over 50%

of cells in these two stimulation paradigms still responded to the AC and showed obvious peaks in the fifth hour (Figures 5C and S10C). Accumulated ERK activation of the first 2-h stimulation was calculated, but no significant statistical difference was found. The average amplitudes of the ERK activation peak from different settings were similar, which indicated that the frequency modulation of ERK activation did not affect the amplitude significantly, however, a tendency seems to exist (Figure S11D). After 2 h of ES, the amplitude of ERK activation appeared to decrease over time.

Our result is similar to frequency modulation of ERK activation achieved using pulsed growth factor stimulation with elegantly designed microfluidics device, in which a sophisticated perfusion system is needed to add and washout EGF at defined time intervals (Ryu et al., 2015). Periodical AC stimulation achieved frequency modulation of synchronized ERK activation with less heterogeneity, and easier control of stimulation duration, magnitude, on-off cycle, and many other parameters (Albeck et al., 2013). No significant cell damage was induced by the repeated AC stimulations with all conditions (Figure S12). The electrical approach appears to be able to generate a robust, easy-to-control, and synchronized frequency modulation of intracellular signaling.

The mechanisms by which AC stimulation activates ERK are not yet fully understood. Our recent work has discovered that the AC EFs specifically act upon phosphorylation sites of EGF receptors to induce ERK activation (Guo et al., 2019). Similar to growth factor pulses (addition-washout), multi-pulse AC stimulation triggered well-resolved ERK activity oscillations with amplitude, duration, frequency, and other parameters that might be controlled more conveniently. Combining different parameters of AC stimulation, or even combining AC with chemical stimuli (EGF for example) would be expected to enable the induction of broader dynamic patterns of ERK activation. We also noticed that 2′ AC pulses are nearly as effective as 3′ GF stimulation with less desensitization. Optogenetic approaches are also effective to regulate ERK dynamics by taking advantage of the high temporal and spatial resolution of optogenetic control. Genetic engineering of a light-gated switch to drive Ras/ERK activation has gained great applications in both *in vitro* and *in vivo* control of ERK activation dynamics (Bugaj et al., 2018; Johnson et al., 2017; Toettcher et al., 2013). However, optogenetic tools require genetic manipulation of the target cells, which may limit their use in clinical applications.

Electrical modulation of ERK dynamics promoted differentiation of PC12 cells

To determine possible functional outcomes of modulation of ERK activation dynamics, we expressed ERKTR in PC12 cells and subjected the cells to a train of AC stimulation. We analyzed ERK activation dynamics and cell fate determination. It is well established that different ERK activation dynamics in PC12 dictate whether cells choose to differentiate or not (Avraham and Yarden, 2011; Marshall, 1995; Ryu et al., 2015).

We co-transfected ERKTR and a nuclear fluorescent protein in PC12 cells to confirm the ERK responses upon AC stimulations. As expected, PC12 cells responded to a train of short AC stimulation in a way that was comparable to MCF10A cells (Figure 6; Video S8). Before stimulation, ERKTR was diffusely distributed in the entire cell with a concentrated expression level in the nucleus (Figure 6A). A 2′ AC stimulation (28V/cm, 500Hz, and bipolar square wave) induced rapid translocations of ERKTR signals from the nucleus to the cytosol which is similar to the responses of MCF10A (Figure 6; Video S8. Compare with Figures 4 and 5). Exposure to a train of 2′ AC with a 20′ interval resulted in robust ERK activation waves in PC12 cells (Figures 6B–6E).

We noticed that electro-activation of ERK lasted longer in PC12 cells than in MCF10A cells, which suggest that the signaling networks these two types of cells are different. This is in consistent with ERK activation induced by EGF that in MCF10A cells, EGF leads to multiple stochastic pulses of ERK, whereas in PC12 cells, EGF induces one ERK activity pulse (Vaudry et al., 2002; Worster et al., 2012). Direct translation of what found in MCF10A to PC12 needs to be tested and interpreted with caution.

At the single-cell level, more oscillatory ERK activity trajectories were observed in PC12 cells (Figures 6B and 6C), indicating that AC-stimulation produces heterogeneous cell responses that may lead to less adaptive ERK activities. And indeed, at population level, MCF10A showed adaptive responses (Figure 5), whereas PC12 displayed a larger number of sustained ERK activity trajectories after AC stimulation (Figure 6). This may result from different strengths of feedback controls of ERK responses within different cell types (Albeck et al., 2013; Markevich et al., 2004).

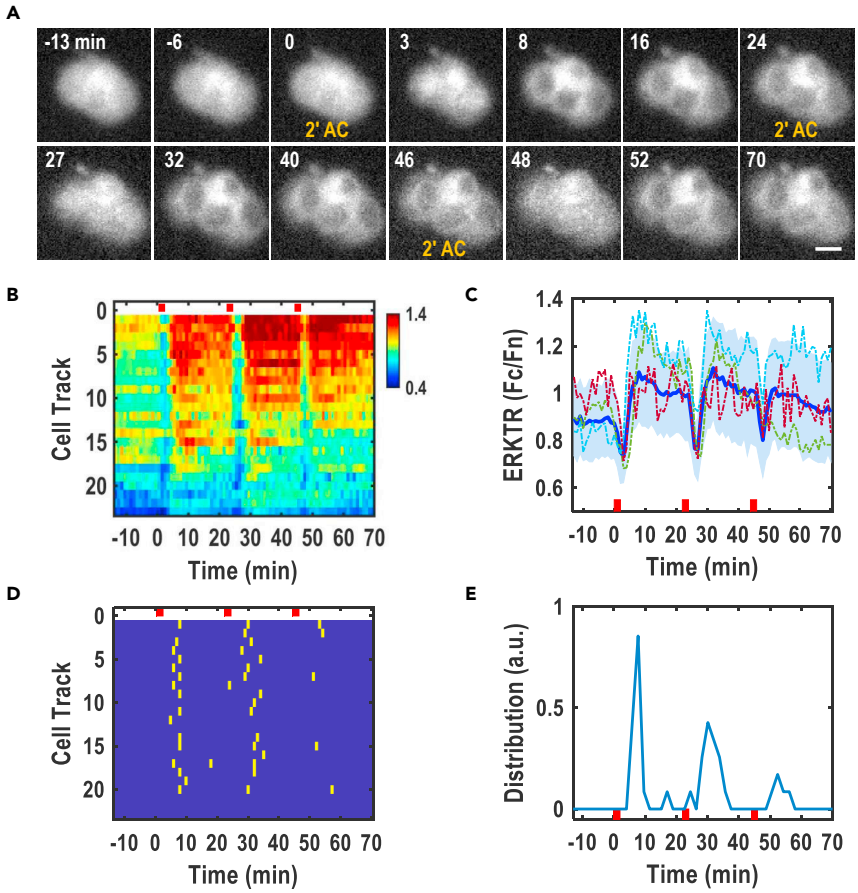

Figure 6. Train stimulation of AC modulated ERK dynamics in PC12 cells

(A) ERK activation in PC12 cells expressing ERKTR by multiple 2′ AC stimulation.

(B) Composite heatmap over time showing ERK dynamics of individual cells in each line as quantified by Fc/Fn.

(C) Mean ERK activation (thick blue line) (from b, n = 23 cells), with the SD range shown in light blue shade. ERK trajectories of three random cells are also shown (thin dotted curves).

(D) Peak map of ERK activation identified automatically from b. Each row represents one cell. Yellow dots indicate ERK peaks.

(E) ERK peak distribution quantified from the peak points in (D). Note: Red thick bars indicate the duration of electric stimulation. EF = 28V/cm (RMS), 500Hz, bipolar square wave. Scale bars, 20 μm.

To determine the effect of AC stimulation on cell fate regulation by modulating ERK dynamics, we next subjected PC12 cells to trains of AC EFs for three days and analyzed the neurite outgrowth. Based on our previous findings, we tested three stimulation schemes: 2′ on/10′ off, 2′ on/20′ off, and 2′ on/60′ off. Cells maintained in culture medium supplied with 0.5% FBS and in medium containing 50 ng/mL NGF without AC stimulation were used as negative and positive controls, respectively. In the negative control cultures, cells remain undifferentiated (Figure 7A). Cells in the positive control cultures with 50 ng/mL NGF addition showed noticeable neurite outgrowth 24 h after NGF addition and more obvious neurite growth 48 h later (Figures 7A, S13, and S14).

Trains of AC stimulation with different stimulation regimes (on/off: 2′/10′, 2′/20′, 2′/60′) induced obvious neurite growth on PC12 cells (Figures 7, S13, and S14). After 3 days of stimulation, AC pulses enhanced neurite outgrowth lengths as well as neurite numbers (Figures 7B and 7C), albeit not as effectively as NGF. Stimulation regimes of 2′/10′ and 2′/20′ appeared to be more effective. 2′/20′ AC regime induced significantly longer mean neurite length per cell after 3 days when compared to the negative control, while the number of neurites for each cell in 2′/10′ and 2′/20′ groups were significantly higher than the negative control (Figure 7B). We also quantified the differentiation rate, which showed a similar trend (Figures 7D and S14D). To further determine the requirement of ERK activation in AC-induced cell differentiation, we

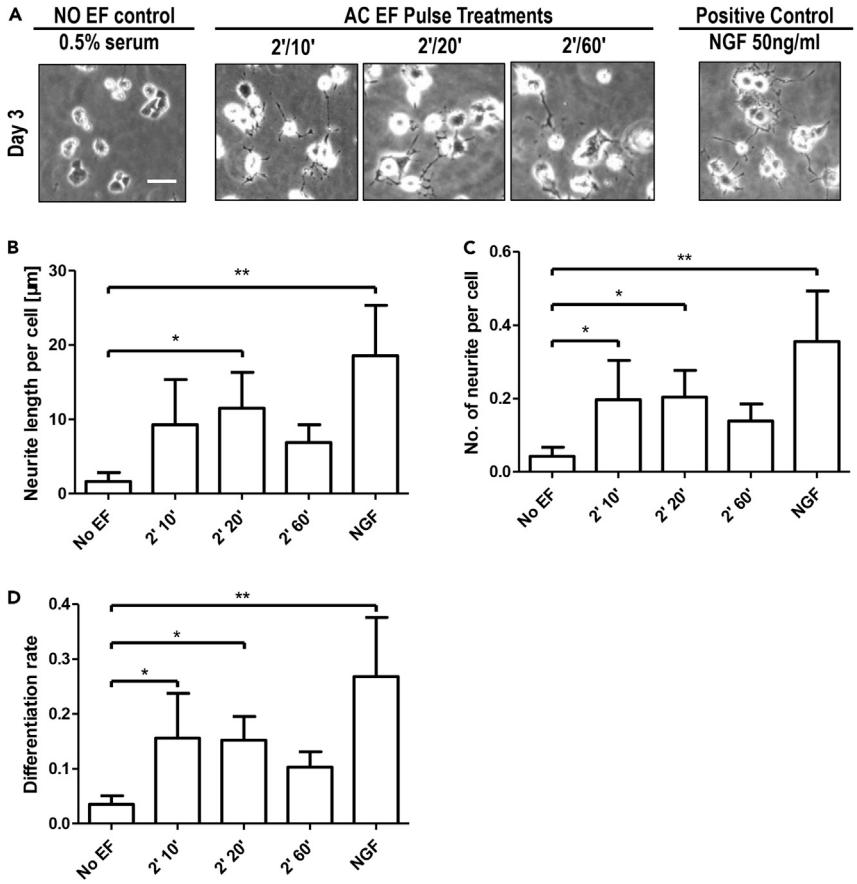

Figure 7. AC stimulation promoted PC12 cell differentiation

(A) Representative phase-contrast images of PC12 cells with/without stimulation after 3 days.

(B–D) Quantification of neuronal differentiation of PC12 cells. (B) Neurite outgrowth length per cell. (C) No. of neurite per cell. (D) Differentiation rate of PC12 cells after 3-days stimulation. At least 500 cells were quantified in 2 independent experiments for each condition. Only neurites with lengths greater than 20 μm were taken into account. Data are shown as mean ± SD. *$p < 0.05$, one-way ANOVA followed by Dunnett's test, compared with the no EF control. Scale bars, 50 μm.

treated PC12 using ERK inhibition (MEK/ERK inhibitor, PD325901). PD325901 abolished AC stimulation-induced cell differentiation (Figure S15).

In summary, we demonstrated that precisely controlled trains of short AC stimulation induced robustly and quantitatively defined ERK activation dynamics. Such ERK dynamic regulation was capable of determining cell fate. AC electric stimulation has some distinct advantages that complement other available means to regulate ERK activation dynamics. Electrical stimulation is relatively easier to apply. Voltage, waveform, frequency, on-and-off switch, and duration can be precisely controlled. No exogenous chemicals or genetic manipulation are needed. AC stimulation thus can be used comparably easily *in vivo*, where electrodes can be placed and avoid substantial electro-hydrolysis and electrochemical reactions typically associated with DC. The electrical approach reported here will be a powerful biomedical engineering tool, complementary to microfluidics and optogenetic approaches.

Limitations of the study

Regarding the electrical regulation of intracellular signaling activities, one key question remaining is how cells sense electrical stimulations. Although we proposed in our previous studies (Guo et al., 2019; Pu et al., 2007) that the coupling between EFs and ERK may initiated by ligand-independent EGFR phosphorylation followed by the activation of EGFR-Ras-ERK signaling pathway, the sensor molecules for electric fields in cells remain elusive and further investigations are needed. Another notable

limitation of this study is that we have not yet quantified other signaling pathways beside ERK. Molecular specificity similar to optogenetics-induced-signaling and microfluidics-induced-signaling cannot be conferred to electric stimulation. Regardless of molecular specificity, controlled cell fate can be achieved through similar signaling dynamics. These approaches together, or applied individually depending on circumstances, are expected to contribute significantly to the understanding of mechanisms, *in vivo* applications, and eventually, use in clinics through regulation of intracellular signaling dynamics.

STAR★METHODS

Detailed methods are provided in the online version of this paper and include the following:

- KEY RESOURCES TABLE
- RESOURCE AVAILABILITY
  - Lead contact
  - Materials availability
  - Data and code availability
- EXPERIMENTAL MODEL AND SUBJECT DETAILS
  - Reporter cell line construction
- METHOD DETAILS
  - Cell culture
  - Fabrication of the EF device
  - AC stimuli application
  - Live cell imaging
  - Pc12 differentiation
- QUANTIFICATION AND STATISTICAL ANALYSIS
  - ERKTR image analysis
  - Peak identification
  - Quantification of PC12 cell differentiation
  - Statistical analysis

SUPPLEMENTAL INFORMATION

Supplemental information can be found online at https://doi.org/10.1016/j.isci.2021.103240.

ACKNOWLEDGMENTS

This work is supported by the AFOSR-MURI grant FA9550-16-1-0052, and NIH 1R01EY019101. Work in Zhao Laboratory is also supported by NEI Core Grant (P-30 EY012576, PI. Jack Werner), the Research to Prevent Blindness, Inc. JA is supported by NIH R01GM115650. The authors would like to thank Heather Blizard from the Albeck lab for assistance on electrotransfection.

AUTHOR CONTRIBUTIONS

L.G., K.Z., and M.Z. developed the conception and designed the study, J.A. provided the MCF10A cell line and ERK reporter used in the research. L.G. and K.Z. collected most of the ERK modulation data and drafted the manuscript with help from all authors. L.G., M.P., and P. T. quantified the ERK dynamics. K.Z. did the transfection and ERK dynamic regulation experiment on PC12 cells. L.G. did the PC12 differentiation experiments, K.Z. and A.C. performed differentiation analysis. Q.Q. and W. L. contributed to the interpretation of the results. K.Z. finalized the manuscript with contributions from all authors.

DECLARATION OF INTERESTS

Min Zhao, John Albeck, Quan Qing and Liang Guo are named inventors with Houpu Li of a U.S. Patent application no. 16/675,127, filed November 5, 2019. Cell signaling pathway activation by local AC electric field. The patent is under consideration. The manuscript used some techniques described in the patent to regulate signaling dynamics. Arizona State University and University of California are patent applicants.

INCLUSION AND DIVERSITY

We worked to ensure diversity in experimental samples through the selection of the cell lines. The author list of this paper includes contributors from the location where the research was conducted who participated in the data collection, design, analysis, and/or interpretation of the work.

Received: August 30, 2021
Revised: September 18, 2021
Accepted: October 5, 2021
Published: November 19, 2021

REFERENCES

Albeck, J.G., Mills, G.B., and Brugge, J.S. (2013). Frequency-modulated pulses of ERK activity transmit quantitative proliferation signals. Mol. Cell *49*, 249–261. https://doi.org/10.1016/j.molcel.2012.11.002.

Allan, L.A., Morrice, N., Brady, S., Magee, G., Pathak, S., and Clarke, P.R. (2003). Inhibition of caspase-9 through phosphorylation at Thr 125 by ERK MAPK. Nat. Cell Biol. *5*, 647–654. https://doi.org/10.1038/ncb1005.

Aoki, K., Kondo, Y., Naoki, H., Hiratsuka, T., Itoh, R.E., and Matsuda, M. (2017). Propagating wave of ERK activation orients collective cell migration. Dev. Cell *43*, 305–317.e305. https://doi.org/10.1016/j.devcel.2017.10.016.

Avraham, R., and Yarden, Y. (2011). Feedback regulation of EGFR signalling: decision making by early and delayed loops. Nat. Rev. Mol. Cell Biol. *12*, 104–117. https://doi.org/10.1038/nrm3048.

Behar, M., and Hoffmann, A. (2010). Understanding the temporal codes of intracellular signals. Curr. Opin. Genet. Dev. *20*, 684–693. https://doi.org/10.1016/j.gde.2010.09.007.

Bugaj, L.J., Sabnis, A.J., Mitchell, A., Garbarino, J.E., Toettcher, J.E., Bivona, T.G., and Lim, W.A. (2018). Cancer mutations and targeted drugs can disrupt dynamic signal encoding by the Ras-Erk pathway. Science *361*. https://doi.org/10.1126/science.aao3048.

Cook, B., Proctor, D., Bromberg, R., LaPointe, N.E., Feinstein, S.C., and Wilson, L. (2017). Digital quantification of neurite outgrowth and retraction by phase-contrast microscopy: a tau perspective. Methods Cell Biol. *141*, 217–228. https://doi.org/10.1016/bs.mcb.2017.06.003.

Deneke, V.E., and Di Talia, S. (2018). Chemical waves in cell and developmental biology. J. Cell Biol. *217*, 1193–1204. https://doi.org/10.1083/jcb.201701158.

Guo, L., Li, H., Wang, Y., Li, Z., Albeck, J., Zhao, M., and Qing, Q. (2019). Controlling ERK activation dynamics in mammary epithelial cells with alternating electric fields through microelectrodes. Nano Lett. *19*, 7526–7533. https://doi.org/10.1021/acs.nanolett.9b03411.

Guo, L., Xu, C., Li, D., Zheng, X., Tang, J., Bu, J., Sun, H., Yang, Z., Sun, W., and Yu, X. (2015). Calcium ion flow permeates cells through SOCs to promote cathode-directed galvanotaxis. PLoS One *10*, e0139865. https://doi.org/10.1371/journal.pone.0139865.

Hansen, A.S., and O'Shea, E.K. (2013). Promoter decoding of transcription factor dynamics involves a trade-off between noise and control of gene expression. Mol. Syst. Biol. *9*, 704. https://doi.org/10.1038/msb.2013.56.

Hansen, A.S., and O'Shea, E.K. (2016). Encoding four gene expression programs in the activation dynamics of a single transcription factor. Curr. Biol. *26*, R269–R271. https://doi.org/10.1016/j.cub.2016.02.058.

Hao, N., and O'Shea, E.K. (2011). Signal-dependent dynamics of transcription factor translocation controls gene expression. Nat. Struct. Mol. Biol. *19*, 31–39. https://doi.org/10.1038/nsmb.2192.

Jaqaman, K., Loerke, D., Mettlen, M., Kuwata, H., Grinstein, S., Schmid, S.L., and Danuser, G. (2008). Robust single-particle tracking in live-cell time-lapse sequences. Nat. Methods *5*, 695–702. https://doi.org/10.1038/nmeth.1237.

Johnson, H.E., Goyal, Y., Pannucci, N.L., Schupbach, T., Shvartsman, S.Y., and Toettcher, J.E. (2017). The spatiotemporal limits of developmental Erk signaling. Dev. Cell *40*, 185–192. https://doi.org/10.1016/j.devcel.2016.12.002.

Klemke, R.L., Cai, S., Giannini, A.L., Gallagher, P.J., de Lanerolle, P., and Cheresh, D.A. (1997). Regulation of cell motility by mitogen-activated protein kinase. J. Cell Biol. *137*, 481–492.

Lai, C.F., Chaudhary, L., Fausto, A., Halstead, L.R., Ory, D.S., Avioli, L.V., and Cheng, S.L. (2001). Erk is essential for growth, differentiation, integrin expression, and cell function in human osteoblastic cells. J. Biol. Chem. *276*, 14443–14450. https://doi.org/10.1074/jbc.M010021200.

Luciano, F., Jacquel, A., Colosetti, P., Herrant, M., Cagnol, S., Pages, G., and Auberger, P. (2003). Phosphorylation of Bim-EL by Erk1/2 on serine 69 promotes its degradation via the proteasome pathway and regulates its proapoptotic function. Oncogene *22*, 6785–6793. https://doi.org/10.1038/sj.onc.1206792.

Markevich, N.I., Hoek, J.B., and Kholodenko, B.N. (2004). Signaling switches and bistability arising from multisite phosphorylation in protein kinase cascades. J. Cell Biol. *164*, 353–359. https://doi.org/10.1083/jcb.200308060.

Marshall, C.J. (1995). Specificity of receptor tyrosine kinase signaling: transient versus sustained extracellular signal-regulated kinase activation. Cell *80*, 179–185.

Micali, G., Aquino, G., Richards, D.M., and Endres, R.G. (2015). Accurate encoding and decoding by single cells: amplitude versus frequency modulation. PLoS Comput. Biol. *11*, e1004222. https://doi.org/10.1371/journal.pcbi.1004222.

Murphy, L.O., Smith, S., Chen, R.H., Fingar, D.C., and Blenis, J. (2002). Molecular interpretation of ERK signal duration by immediate early gene products. Nat. Cell Biol. *4*, 556–564. https://doi.org/10.1038/ncb822.

Pargett, M., Gillies, T.E., Teragawa, C.K., Sparta, B., and Albeck, J.G. (2017). Single-cell imaging of ERK signaling using fluorescent biosensors. Methods Mol. Biol. *1636*, 35–59. https://doi.org/10.1007/978-1-4939-7154-1_3.

Pu, J., McCaig, C.D., Cao, L., Zhao, Z., Segall, J.E., and Zhao, M. (2007). EGF receptor signalling is essential for electric-field-directed migration of breast cancer cells. J. Cell Sci. *120*, 3395–3403. https://doi.org/10.1242/jcs.002774.

Purvis, J.E., and Lahav, G. (2013). Encoding and decoding cellular information through signaling dynamics. Cell *152*, 945–956. https://doi.org/10.1016/j.cell.2013.02.005.

Ravindran, P.T., and Wilson, M.Z. (2018). Lighting up cancer dynamics. Trends Cancer *4*, 657–659. https://doi.org/10.1016/j.trecan.2018.06.001.

Regot, S., Hughey, J.J., Bajar, B.T., Carrasco, S., and Covert, M.W. (2014). High-sensitivity measurements of multiple kinase activities in live single cells. Cell *157*, 1724–1734. https://doi.org/10.1016/j.cell.2014.04.039.

Roux, P.P., and Blenis, J. (2004). ERK and p38 MAPK-activated protein kinases: a family of protein kinases with diverse biological functions. Microbiol. Mol. Biol. Rev. *68*, 320–344. https://doi.org/10.1128/MMBR.68.2.320-344.2004.

Ryu, H., Chung, M., Dobrzynski, M., Fey, D., Blum, Y., Lee, S.S., Peter, M., Kholodenko, B.N., Jeon, N.L., and Pertz, O. (2015). Frequency modulation of ERK activation dynamics rewires cell fate. Mol. Syst. Biol. *11*, 838. https://doi.org/10.15252/msb.20156458.

Sparta, B., Pargett, M., Minguet, M., Distor, K., Bell, G., and Albeck, J.G. (2015). Receptor level mechanisms are required for epidermal growth factor (EGF)-stimulated extracellular signal-regulated kinase (ERK) activity pulses. J. Biol.

Chem. *290*, 24784–24792. https://doi.org/10.1074/jbc.M115.662247.

Toettcher, J.E., Weiner, O.D., and Lim, W.A. (2013). Using optogenetics to interrogate the dynamic control of signal transmission by the Ras/Erk module. Cell *155*, 1422–1434. https://doi.org/10.1016/j.cell.2013.11.004.

Vaudry, D., Chen, Y., Ravni, A., Hamelink, C., Elkahloun, A.G., and Eiden, L.E. (2002). Analysis of the PC12 cell transcriptome after differentiation with pituitary adenylate cyclase-activating polypeptide (PACAP). J. Neurochem. *83*, 1272–1284. https://doi.org/10.1046/j.1471-4159.2002.01242.x.

Wilson, M.Z., Ravindran, P.T., Lim, W.A., and Toettcher, J.E. (2017). Tracing information flow from Erk to target gene induction reveals mechanisms of dynamic and combinatorial control. Mol. Cell *67*, 757–769.e755. https://doi.org/10.1016/j.molcel.2017.07.016.

Worster, D.T., Schmelzle, T., Solimini, N.L., Lightcap, E.S., Millard, B., Mills, G.B., Brugge, J.S., and Albeck, J.G. (2012). Akt and ERK control the proliferative response of mammary epithelial cells to the growth factors IGF-1 and EGF through the cell cycle inhibitor p57Kip2. Sci. Signal. *5*, ra19. https://doi.org/10.1126/scisignal.2001986.

Wortzel, I., and Seger, R. (2011). The ERK cascade: distinct functions within various subcellular organelles. Genes Cancer *2*, 195–209. https://doi.org/10.1177/1947601911407328.

Zhu, K., Takada, Y., Nakajima, K., Sun, Y., Jiang, J., Zhang, Y., Zeng, Q., Takada, Y., and Zhao, M. (2019). Expression of integrins to control migration direction of electrotaxis. FASEB J. *33*, 9131–9141. https://doi.org/10.1096/fj.201802657R.

STAR★METHODS

KEY RESOURCES TABLE

REAGENT or RESOURCE	SOURCE	IDENTIFIER
Chemicals, peptides, and recombinant proteins		
EGF	Thermo Fisher Scientific	Cat#PHG0311
NGF	Thermo Fisher Scientific	Cat#11050HNAC25
Horse Serum	Thermo Fisher Scientific	Cat#26050088
Insulin	Sigma-Aldrich	Cat#I9278
Cholera Toxin	Sigma-Aldrich	Cat#C8052
Collagen IV	Sigma-Aldrich	Cat#C5533
Hydrocortisone	Sigma-Aldrich	Cat#H0888
PDMS	Dow Corning	Cat#0008691565
Gefitinib	Selleck Biochemicals	Cat#S1025
PD325901 MEK inhibitor	Cell signaling	Cat#79241S
Experimental models: cell lines		
MCF10A	ATCC	CRL-10317; RRID:CVCL_0598
PC12	ATCC	CRL-1721; RRID:CVCL_0481
Recombinant DNA		
Plasmid: EKAR3-FRET	Sparta et al., 2015	N/A
Plasmid: ERKTR-mCherry	Sparta et al., 2015	N/A
Software and algorithms		
Metamorph NX	Molecular Devices	MetaMorph NX 2.5, https://www.moleculardevices.com/products/cellular-imaging-systems/acquisition-and-analysis-software/metamorph-microscopy
MatLab	MathWorks	MATLAB R2017a, https://www.mathworks.com/products/matlab.html
ImageJ	Image J	https://imagej.nih.gov/ij/
GraphPad Prism	GraphPad	GraphPad Prism 7, https://www.graphpad.com/scientific-software/prism/

RESOURCE AVAILABILITY

Lead contact

Further information and requests for resources and reagents should be directed to and will be fulfilled by the lead contact Min Zhao (minzhao@ucdavis.edu).

Materials availability

This study did not generate new unique reagents.

Data and code availability

- All data reported in this paper will be shared by the lead contact upon request.
- This paper does not report original code.
- Any additional information required to reanalyze the data reported in this paper is available from the lead contact upon request.

EXPERIMENTAL MODEL AND SUBJECT DETAILS

Reporter cell line construction

MCF10-A cell line stably expressing ERKTR-mCherry and EKAR3-FRET was generated by retroviral gene transfer and PiggyBac transposase system as previously described (Pargett et al., 2017; Sparta et al., 2015). The PC12 cell line was co-transfected ERKTR and EKAR3 by electroporation. Cells were then seeded in 12 well-plates coated with Collagen IV. 2 μg/mL puromycin was added into the cell culture medium for antibiotic selection. 2-4 weeks after selection, cell colonies were collected and dissociated by treating with Accutase solution (Sigma A6964). Monoclonal cell populations were isolated by limiting dilution. Briefly, PC12 cell clumps were broken up into individual cells by passing several times through a serological pipet or by passing through a 0.40 μm cell strainer mesh. Cell concentration was quantitated with a cell counter. This homogenized cell solution was then diluted by fresh cell culture medium at a concentration of 5 cells/ml. 100 μL diluted cell solution was transferred into each well of a 96-well plate to ensure that each well receives no more than one single cell. Cells were left undisturbed in an incubator for 14 days and then scanned under a fluorescence microscope to select monoclonal cell populations with both reporters expressed.

METHOD DETAILS

Cell culture

MCF10A cells were cultured in Dulbecco's modified Eagle's medium (DMEM)/F-12, supplemented with 5% horse serum, EGF (20 ng/ml), insulin (10 mg/ml), hydrocortisone (0.5 ng/ml), cholera toxin (100 ng/ml), penicillin (50 U/ml)), and streptomycin (50 mg/ml). PC12 cells were routinely cultured in Roswell Park Memorial Institute (RPMI) 1640 Medium supplemented with 10% heat-inactivated horse serum, 5% fetal bovine serum, and 1% penicillin/streptomycin.

Fabrication of the EF device

The AC stimulation chambers were constructed as previously described with some modifications (Guo et al., 2015; Zhu et al., 2019). Briefly, manually-cut glass strips (20 mm × 1 mm × 0.17 mm) were attached to the base of a 10 cm Petri dish (Corning, CLS430167) as the mold of cell chambers for AC stimulation (20 mm × 1 mm × 0.17 mm). PDMS prepolymer was mixed with curing reagent at a 10:1 ratio and degassed in a vacuum chamber for 60 min and poured onto the Petri dish with glass strips on the base to form a layer of 3-5 mm thick. PDMS was then cured by heating to 90°C for 30 min. The PDMS layer was gently peeled off from the Petri dish and cut into the shape as shown in Figure 1A by a blade. 2 holes were punched in the PDMS layer connecting with the cell chamber to form reservoirs for maintaining the medium. After sterilization, each chamber was sealed in a 10mm Petri dish. Water/PBS was added to the dish outside the PDMS chamber to maintain humidity. The dish was then covered with a customized lid with two secured silver electrodes to deliver EF stimulation and a pair of reference electrodes to monitor the voltage in the stimulation chamber.

AC stimuli application

One day before EF stimulation, MCF10A (7×10^6 cells/ml) or PC12 (1×10^6 cells/ml) cell suspensions were seeded into the stimulation chamber and incubated 2 hours at 37°C for full attachment. PC12 cells were seeded on chambers pre-coated with 50 μg/ml of Collagen IV for 1 hour. The fresh culture medium was then added to the chamber to washout unattached cells. Cells were then incubated overnight in 5% CO_2 at 37°C.

EFs were delivered through Ag/AgCl electrodes directly through the medium. AC stimulation of all the frequencies and waveforms were generated by a programmable AC power supply (GW Instek, APS-7100). A programmable digital time relay controlled the delivery of the EF stimulation generated from the AC power source to achieve interval AC stimulation. The electric fields were monitored by an oscilloscope or digital multimeter in all experiments.

Live cell imaging

All fluorescence imaging experiments were performed on a Zeiss Axio Observer Z1 microscope with a 10x EC Plan-Neofluar (NA 0.3) objective controlled by the Metamorph software (Molecular Devices). Images were recorded by a QImaging Retiga R6 Large Field of View Scientific CCD camera at 16-bit depth. Images of the phase-contrast channel, nucleus channel, and ERKTR channel acquired sequentially using filter wheels. Autofocus was used at the phase-contrast channel by Metamorph software throughout the

experiments. The following filter sets were used: nucleus channel (YFP), 46 HE; ERKTR channel (RFP), 43HE. Exposure times were 400 ms for RFP channel and 700 ms for YFP, and images were acquired every 1-3 min at binning 2 × 2.

To minimize the background fluorescence, 2 h prior to cell imaging the culture medium was replaced by a low fluorescence medium consisting of DMEM/F12 lacking phenol red and supplemented with hydrocortisone (0.5 ng/ml), cholera toxin (100 ng/ml), and 1% penicillin/streptomycin for MCF10A cell line. The prepared chamber was mounted on the microscope stage and was connected to the AC power supply controlled by a time relay and voltage meter. An incubator was used to maintain the culture at 37°C in 5% CO_2 throughout the experiments.

Pc12 differentiation

PC12 cells were seeded into the stimulation chambers that pre-coated with collagen IV and incubated overnight prior to experiments. 2 hours before AC stimulation, the cell culture medium was changed to a differentiation medium consisting of DMEM, 0.5% FBS, and 1% penicillin/streptomycin. The prepared chamber was mounted on the microscope stage. AC power supply controlled by timer relay was connected to each channel as previously described. Multi-interval AC stimulations were delivered to PC12 cells for 3 days. 28 V/cm, 500 Hz, bipolar square wave AC EF was applied. The AC were paused for 1 hour after each 2 hours of stimulation to minimize desensitization. To prevent overheating caused by the AC currents which may affect cell differentiation, the temperature in the incubator was set to 35°C. The medium in the chambers and the water in the gap between PDMS chamber and Petri dish wall were refreshed every day. The negative (no AC pulse) and positive (50 ng/ml NGF without AC stimulation) controls were performed in the same condition with AC groups. Phase-contrast images were recorded to evaluate cell differentiation.

QUANTIFICATION AND STATISTICAL ANALYSIS

ERKTR image analysis

Raw images were converted to TIFF stacks by ImageJ and imported to MATLAB for image segmentation, tracking, and quantitation as described previously (Pargett et al., 2017). Briefly, after background subtraction, the nuclear region was identified based on the nuclear localization of EKAR3 which contains a nuclear import sequence. Individual cell tracking was achieved using the u-track algorithm (Jaqaman et al., 2008) to the automated selection of edge-based contours. The cytosolic region was defined as the neighboring 7-pixel outside the nuclear region. Cell ERKTR level was calculated as Fc/Fn, where Fc and Fn stand for the RFP fluorescence intensity of cytosol and nucleus, respectively.

Peak identification

Trajectories of ERK activation in individual cells in Fc/Fn value were processed to identify the ERK activation peaks by a custom MATLAB program. To be robust to noise and baseline drift, pulses were defined by where the intensity rises/falls across both a minimum peak threshold and maximum valley threshold, defined as 33% and 60% of the local signal of the rest condition.

Quantification of PC12 cell differentiation

For each cell line, over 500 cells were analyzed. Only distinguishable single cells were counted in. Cell clumps were excluded from the analysis. Neurite length and number of neurites for each condition were quantified by using ImageJ software from the National Institutes of Health (https://imagej.nih.gov/ij/) with NeuronJ plugin as previously described (Cook et al., 2017). Briefly, each neurite was traced from the origin of the neurite at the cell body to the end by automatic detection or manually tracing. The length of neurite was computed by NeuronJ. Neurite length per cell, number of neurites per cell, and differentiation rate were then calculated to evaluate PC12 cell differentiation.

Statistical analysis

For all the experiments, at least two independent experimental replicates were performed. For visual clarity, figures show individual replicate experiments, and we verified similar trends in the replicate. p value was set at 0.05 for rejecting null hypotheses. MATLAB and GraphPad Prism were used for all the statistical and computational tasks.